Disaster Protection in Inter-DataCenter Networks leveraging Cooperative Storage

Yuanhao Liu, Fen Zhou, *Senior Member, IEEE,* Cao Chen, Zuqing Zhu, *Senior Member, IEEE,* Tao Shang, and Juan-Manuel Torres-Moreno

***Abstract*—Natural disasters have challenged the survivability of Elastic Optical Inter-DataCenter Networks (EO-DCNs), and it is urgent to establish efficient disaster protection schemes. In this paper, we investigate the disaster-resilient service provisioning problem leveraging cooperative storage system (CSS). Instead of mirrored content backup on a single DC, our proposed CSS partitions a required content into no less than three fragments if possible, each of which is then stored on a DC located in different disaster zones. Accordingly, multi-path routing with the adaptive number of working paths to distinct DCs is employed to serve each request, while a protection path is computed to protect against a disaster failure. Our main objective is to jointly minimize the spectrum usage and maximal occupied frequency slot index (MOFI) subject to disaster resilience. Besides, we also expect to cut the content storage space. To this end, we propose for the first time a CSS-based dedicated end-to-content path protection (CDP), which allows service provisioning through multiple paths with the adaptive number of paths rather than a single path. This consequently reduces at least half of the reserved spectrum on the protection path. To find the optimal CDP strategy, we formulate the studied problem as an integer linear program (ILP) and then propose a fast heuristic algorithm. Observing the trade-off between the spectrum usage and content storage space, we further design a maximum-CDP (M-CDP), which generates the maximum number of working paths to reduce the content storage space. Simulations are conducted to compare the proposed schemes with the traditional protection strategy using mirrored storage and single-path routing. Numerical results demonstrate that the proposed CSS-based protection schemes enable to cut up to 21.6% of the spectrum usage and 15% of the content storage space.**

***Index Terms*—Inter-DataCenter Networks, Elastic Optical Networks, Disaster resilience, Cooperative Storage System (CSS)**

A preliminary version of this work has been accepted by IEEE Globecom conference 2020 [1]. The work is partially supported by the Campus France Eiffel Excellence Scholarship (No.P745849E), China Scholarship Council (202006960046), Campus France PHC Cai Yuanpei 2019 project (44016XA), the 863 High Technology Plan of China (2013AA013402), the National Natural Science Foundation of China (61172080, 61771357), Xidian University, China, and the open project (2020GZKF017) of the State Key Laboratory of Advanced Optical Communication Systems and Networks, Shanghai Jiao Tong University, China. *Corresponding author: Fen Zhou.*

Yuanhao Liu is with the State Key Laboratory Integrated Service Networks, School of Telecommunications Engineering, Xidian University, China. He is also with CERI-LIA, Computer Science Laboratory, University of Avignon, France. (email: yuanhao.liu@alumni.univ-avignon.fr).

Fen Zhou is with IMT Lille Douai, Institut Mines-Télécom, Univ. Lille, Center for Digital Systems, France. (email: fen.zhou@imt-lille-douai.fr).

Cao Chen is with CERI-LIA, University of Avignon, France. He is also with the State Key Laboratory of Advanced Optical Communication Systems and Networks, Shanghai Jiao Tong University, China. (email: cao.chen@alumni.univ-avignon.fr)

Zuqing Zhu is with the School of Information Science and Technology, University of Science and Technology of China, China (email: zqzhu@ieee.org).

Tao Shang is with the State Key Laboratory of Integrated Service Networks, School of Telecommunications Engineering, Xidian University, China (email: shtsun_sjtu@hotmail.com).

Juan-Manuel Torres-Moreno is with CERI-LIA, University of Avignon, France (email: juan-manuel.torres@univ-avignon.fr).

I. Introduction

With the high spectrum efficiency and huge spectrum resource capacity, Elastic Optical inter-DataCenter Networks (EO-DCNs) have shown the ability to support big data storage and provide the platform for the deployment of diversified network services and applications [2]–[8]. However, as tens of natural disasters worldwide destroy power systems and subsequently affect optical networks [9], EO-DCNs are facing serious threats from large-scale disasters. A disaster zone (DZ) failure may affect several links and nodes on a large scale and for a relatively long time. Examples include *e.g.*, hurricane Katrina decreased the network usability of the affected area from 99.99% to 85%, which caused severe losses in Louisiana and Mississippi in the Southeastern US in August 2005. The 8.3-magnitude Wenchuan earthquake in May 2008 destroyed 3,897 telecommunication nodes and 28,765 km cables in Sichuan, Gansu, Shaanxi, and other provinces. The interruption of networks may break off the cloud services, 5G, and content distribution services, and it is especially costly for inter-datacenter networks. The downtime of each data center (DC) server may cause a loss of $ 9,000 per minute [10], and such disaster-caused network paralysis may lead to billions of dollars in losses. To maintain the survivability of content delivery in EO-DCNs, anycast technique provides the mechanism of path protection against network failure [11] [12]. When the content or service is required, it is provisioned with several potential DCs and corresponding routing. However, existing protection schemes mostly aim at single link or node failure, which cannot deal with such disaster failure [13]. Hence, there is a strong need to develop protection methods to ensure end-to-end communications in EO-DCNs.

The requirement for huge content storage space also grows rapidly. The amount of Internet data generated will grow to 2,142 ZB in 2035 [14]. Alone the content streaming contributes an overwhelming percentage of Internet traffic, *e.g.* 79% in 2016. To store these data, 597 hyperscale datacenters have been built by the end of 2020. The market size of the internet DC will reach 139.6 billion dollars by the end of 2020 [15]. To reduce the pressure of storage space for DCs, the maximum distance separable (MDS) codes provide a feasible method of building a cooperative storage system (CSS) for EO-DCN, in which content can be encoded and divided into numerous different fragments, and they are then stored spatially in multiple DCs [16]. Through MDS coding, the required content can be decoded/recovered through the coded segments from different DCs. Therefore, a request can be satisfied with the help of the cooperation of multiple DCs holding the coded segment of the requested content. In other words, multiple DCs can be assigned as the primary DCs simultaneously and a distinct working path from the source node to each of these primary DCs is established to serve the request. Besides, a backup DC is also assured to protect any one of the primary DCs. Meanwhile, the multiple working paths and backup path from end to content are generated as DZ-disjoint to protect the services against a single DZ failure. Thus, if any working path is affected by DZ failure, the backup path can be switched on to replace the failed working path, and enough data segments can guarantee the recovery of the required data. Furthermore, the DC assignment together with content partition and placement also needs to be explored.

We aim to design a novel disaster protection scheme in EO-DCNs leveraging CSS and adaptive multi-path routing. The applicable scenarios include cloud service, content delivery, distributed storage, video-on-demand service, etc. We focus on the cooperative dedicated end-to-content backup path protection (CDP) against disaster failure. To support the adaptive multi-path routing for each request with disaster resilience, the contents are partitioned and jointly encoded into several fragments, each of which is then stored on a DC located in different disaster zones. Then, the CDP allows each request provisioned by multi-path routing with the adaptive number of paths. Besides, we observe that the more working paths CDP uses, the smaller content storage space is required. Then, we extend CDP to maximum CDP (M-CDP), which enables us to find the optimal content storage space by using the maximum number of paths. We further explore how network topologies impact system performance. The existing works of disaster protection leverage a single working path and mirrored storage, which clones the whole content on one backup DC. To the best of our knowledge, it is the first time that the CSS and adaptive multi-path routing are employed for disaster protection in EO-DCNs. The contributions of this paper are summarized as follows.

- We propose a novel disaster protection scheme leveraging CSS and adaptive multiple working paths, namely CDP. The studied CDP problem involves DC assignment, content partition and placement, adaptive working/protection paths computation, modulation adaption, as well as spectrum allocation. We formulate the joint problem as an integer linear program (ILP) to jointly minimize the spectrum usage and maximal index of occupied frequency slots index. Meanwhile, the content storage space is also reduced owing to content partition in CSS and multi-path routing.
- To find efficient CDP strategies for large instances, we then propose a heuristic algorithm, namely HCDP, to solve the working/protection path generation, modulation adaption, adaptive multi-paths routing, and spectrum allocation. The solution in the HCDP algorithm is generated greedily first and then optimized globally after, and it uses coloring algorithms to minimize the spectrum resource by decomposing the spectrum conflict.
- Through CDP, we observe that the spectrum utilization performance is not positively related to the number of the working paths [1]. Hence, to further explore the impact of multi-path routing in the CDP, we propose to generate the maximum number of working paths for each request in the CDP scheme, which is then called M-CDP. Simulation results demonstrate that M-CDP provides a better solution on content storage space while using more spectrum resource.
- Finally, we compare two CDP schemes and a traditional scheme using single-path routing and mirrored storage in NSFNET, COST239, and the US Backbone networks. Simulation results demonstrate the significant performance improvement of the proposed methods compared with the traditional protection scheme.

The rest of the paper is organized as follows. Section II first gives the related work. We then present the CDP disaster protection scheme in Section III and formulate it by a joint ILP in Section IV. In Section V, heuristic algorithm, HCDP, is proposed for CDP and M-CDP, respectively, and their performances are evaluated in Section VI. Section VII concludes our paper.

II. Related Work

Several works about disaster protection in optical networks have been published. A fast and coordinated emergency backup system in geographically distributed optical inter-DC networks was proposed in [17] [18], which is triggered in response to a predictable and progressive disaster. A stochastic model named earthquake risk and backbone optical network model was provided in [19], which estimated the impact of earthquake disasters on a backbone optical network. The authors assessed the generic applicability and evaluated the performance of protection, recovery, and topology design scheme irrespective of the varying geographical region and network topology. Research [20] developed a degraded-service-network to maintain the most traffic after disaster failure, and it uses degraded-service tolerance as the parameter to assign the resource to the connections. The RECODIS project [13] was formed to achieve disaster resilience, and the members of its Working Group 1 gave a survey, which summarized different disaster-resilient strategies of wavelength division multiplexing (WDM) optical networks. The concept of disaster in the networks is described as a group of nodes and links, called shared risk group (SRG), in which the disaster failure would destroy the corresponding nodes and links [21] [22]. A framework for the disaster-resilient optical network called FRADIR was designed in [22], in which authors brought together network design, failure modeling, and protection routing. The disaster resilience is achieved via the edge availability values, shared risk link groups list, and dedicated path protection. Authors in [23] presented the disaster recovery layer that enables OpenStack-managed DC workloads, virtual machines and volumes, to be protected and recovered in another DC. Researchers investigated in [24] a joint progressive network and DC recovery, in which the network recovery and DC recovery are conducted in a coordinated manner.

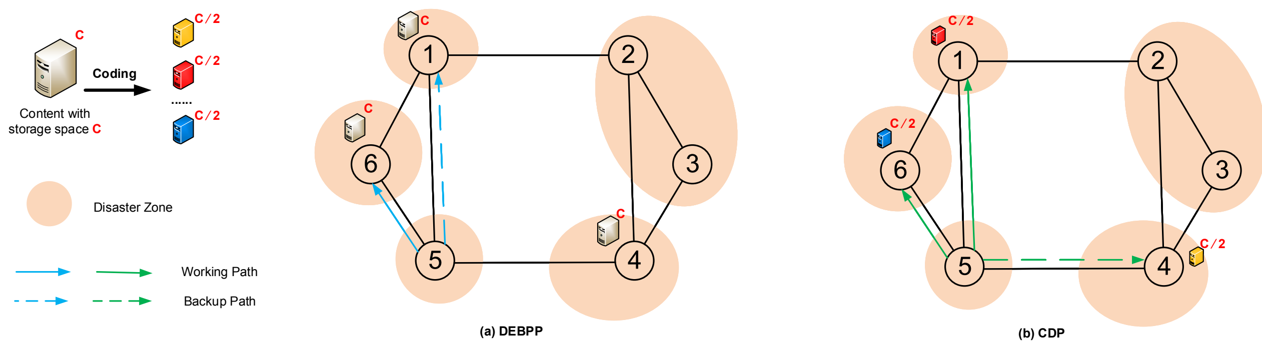

Fig. 1. Solution acquired by DP and CDP with 6-node topology and 5 DZs.

While keeping the disaster resilience for optical networks, several works have been proposed to optimize the network resource. Such disaster protection design was firstly conducted in [25]. The DC placement and content management were explored for EO-DCNs to minimize risk, in which the risk is defined as the expected loss of content. In [26], the algorithms considering both routing and spectrum assignment (RSA) problems for elastic optical networks were proposed, in which the RSA problem has been shown to be NP-hard. The content placement and independent end-to-content paths calculation were explored for the disaster-resilient k-node (edge) content connected EO-DCNs [27]. Cloud service with mirrored storage method in EO-DCNs against disaster failure was investigated in [28] [2], in which the authors proposed both dedicated and shared path protection to maintain disaster resilience. Literature [29] gave a coloring algorithm-based method to generate a conflict graph, which is then used to assign the FSs for all the paths in the network. Diversity and redundancy problem was studied in [30], to achieve network resiliency in terms of availability, reliability, and fault tolerance for service chain provisioning. The existing proposed schemes are based on mirrored replication system, which reserved the same bandwidth on the backup path as the working path, and the storage space is linearly increasing as the number of backup DCs grows, leading to a significant waste of network resource.

As for the network storage system, the CSS has shown better performance in storage efficiency. With erasure codes, the required data is able to be recovered by offering several encoded distinct fragments, which are of the same size in all as the original data. Such codes have a long research history, and typical erasure codes include Reed-Solomon code [31], Low-Density Parity-check Code [32], and so on. Literature [16] first gave the concept of network coding and regenerating code design, and analyzed the trade-off between repair bandwidth and storage space, in which the code with minimal storage space can be regarded as MDS codeAuthors in [33] proposed a survivable virtual network based on network coding, which can achieve the minimal spare capacity for backup links. Erasure codes are also used to achieve content distribution in [34], [35]. Content Distribution was also studied in literature [36], which utilizes Random Linear Network Coding to reduce energy consumption. Paper [37] proposed a partially collaborative repair code to maintain resilience from multiple node failures. In [38], the authors proposed an adaptive multi-cast scheme to optimize the spectrum utilization and blocking ratio for virtual network embedding in elastic optical networks. However, none of the existing works involves disaster protection.

These studies are essential for disaster protection. Previous studies have demonstrated the potential of the CSS on spectrum usage and storage space. However, with respect to all these works, the CSS has never been implemented for disaster protection. The existing disaster protection is only studied based on the traditional mirrored storage system, in which each redundancy of the content in EO-DCNs is a simple clone of the whole original data, and no adaptive multi-path routing is available. Therefore, it is essential to explore CSS-based disaster protection strategies in EO-DCNs.

III. CDP Disaster Protection Scheme

We first give a simple example in Fig. 1 to better illustrate the disaster protection scheme leveraging CSS. We consider a 6-node network with 3 DCs (nodes 1, 4, and 6), 1 content, and 5 DZs, where a request originated from node 5 should be provisioned with the content. For simplicity, we set the modulation format BPSK in this case. Assuming the transmission rate of 100 $Gbps$ is required to transport the content from a DC to node 5. Note that the bandwidth per frequency slot (FS) for EO-DCNs is 12.5 GHz in this work. Fig. 1 (a) draws the solution provided by the **traditional dedicated end-to-content backup path protection (DP)**. The acronym of dedicated end-to-content backup path protection is DEBPP in the works [28] [2]. To ease the readability, We use **DP** referring to it in this work. In this scheme, node 6 is set as the primary DC storing the entire required content, and the content is also mirrored on the backup DC node 1. The request is provisioned with the working path 5-6 and the backup path 5-1, and 8 FSs are utilized on each fiber link of both working and protection paths. While Fig. 1 (b) presents a solution provided by the **scheme leveraging CSS, *i.e.* CDP**. With the help of advanced coding techniques like MDS code [16], the content can be coded into infinitive distinct fragments, and stored on different DCs. This spatial and cooperative storage method has a significant advantage in that the original content can be recovered through the reception of any coded fragments of the same size. Different from the previous solution using only one primary DC, both nodes 1 and 6 are served as the primary working DCs and the backup DC is node 4. Instead of storing

TABLE I
SYSTEM PERFORMANCE IN DP AND CDP.

Schemes	FSs usage	MOFI	Storage Space
DP	16	8	2C
CDP	12	4	3C/2

the whole original content, only the coded fragments are stored on these DCs, and each has a half size of the original one. We can see the request can get the entire required content by establishing two simultaneous working paths from node 5 to nodes 1 and 6. in Fig. 1 (b). Thus, the request is provisioned with two working paths and one backup path, which are DZ-disjoint except for the DZ that the source node is located in. Each working and backup path benefits from the cooperative method to lower its transmission load, which only needs half of the required FSs. Supposing the storage space for the content is C, then CDP allows each DC to cost only $C/2$ in this case. Although the number of total FSs served on the working paths is the same, it is reduced on the backup path from 8 to 4. The spectrum usage, maximal occupied FS index (MOFI), and storage space are then summarized in Table I.

A digraph $G(V, A, D)$ is used in this paper to model the network, where V denotes the set of nodes, A represents the set of symmetric directed links, and D is the set of DCs. For each disaster zone, it may affect several links and nodes. We use $z \in Z$ to denote the affected nodes as well as the links. For any request $r(s_r, z_r, |\mathbf{k}_r|, c_r, \phi_r)$, s_r is the source node, z_r is the disaster zone in which the source node is located, $|\mathbf{k}_r|$ is the number of the working paths to be generated, c_r is the required content, and ϕ_r is the required number of FS using the modulation format BPSK. Note the request will be blocked if a DZ failure destroys more than one generated path simultaneously, including the working path and backup path. To avoid such a situation, we must force the generated paths of each request can not be affected by the same DZ (except z_r). Furthermore, we denote $|\mathbf{k}_r|$ as the number of the path for the request r, and its value is affected by source nodal degree, DZ, content placement, DC locations and etc. In fact, it is not an easy job. The range of $|\mathbf{k}_r|$ can be determined by the *Algorithm* 1 *line 1-21* (see later in Section V). The objective of the studied disaster protection problem is to minimize the weighted sum of the total spectrum usage and the MOFI in the whole network (see later in Section IV, Eq(1)). The objective affects the overall spectrum utilization and network load balancing. The main considerations of each sub-problem can be summarized as follows.

1) **Content partition:**

In this work, a cooperative strategy is proposed to optimize content partition against DZ failure. We assume a content with l size is divided into m fragments of equal size $\frac{l}{m}$. They are jointly encoded into $\tilde{k}$ ($\tilde{k} > m$) distinct fragments, each with $\frac{l}{m}$ size and placed at most K ($\tilde{k} > K > m$) different DCs. Any m distinct fragments would successfully recover the original data. For the request r, the number of fragments on each DC depends on the number of working paths, which should be sufficient for every path that requires the corresponding content. Therefore, the storage space of a content c for CSS in each DC is reduced to $\frac{l}{t_{rkcd}^{max}}$, where t_{rkcd}^{max} is the maximum transmission capacity of the path demanding the content c on DC d. Note that it is possible that the transmission capacity is bigger than the size of the content, due to the granularity of one FS.

2) **DC assignment and content placement:**

Based on the available DC locations and the prior information, DC assignment and content placement are jointly optimized. The prior information for the content is the distribution of the potential source nodes, which contains source node ID, content ID, and the maximal number that the working paths can be generated ($|\mathbf{k}_r|$). In order to ensure content survivability, at least ($k_{r,c}^{max}$) DZ-disjoint DCs should be assigned as the storage DC, where $k_{r,c}^{max}$ is the maximum of $|\mathbf{k}_r|$ among the requests that require the content c. Note that the fragments stored at each DC are distinct from each other in the CDP scheme since they are generated by MDS coding.

3) **Working paths and backup path generation:**

We focus on the failure caused by a single DZ, in which situation the working paths and backup path should be generated as DZ-disjoint (except z_r). Along the paths, the flow conversation should be followed. The dedicated backup path generation method based on CSS is considered, *i.e.* CDP. For CDP, a backup path is generated with dedicated spare capacity, in which the FSs cannot be shared when any two paths use the common link. Note that the failure of z_r would absolutely block the request whose source node is s_r. Thus, this case leads to no solution for the protection of the request r, which is consequently removed from the input request set of our problem.

4) **Modulation adaption**

We consider the modulation level set M consisting of BPSK, QPSK, 8-QAM, and 16-QAM. The granularity of FS is 12.5 GHz in this work. Thus, the protection capacity of one FS with each modulation format is 12.5, 25, 37.5, and 50, in Gbps, respectively [39]. The corresponding maximum transmission reaches of these modulation formats are assumed to be 9,600, 4,800, 2,400, and 1,200, in km, respectively [40]. Each path should be set as the maximum transmission rate depending on its path length since a higher modulation format can provide the provisioning with less spectrum usage.

5) **Adaptive multi-path routing**

For the requests supporting multiple working paths generation, we assign the first path as the working path and the last path as the backup path. The rest paths are automatically selected for the minimum objective. Assuming $|\mathbf{k}_r|$ paths are generated for the request r, then any $|\mathbf{k}_r| - 1$ paths should provide sufficient transmission capacity to serve the request.

6) **Spectrum allocation:**

For each path, the spectrum is allocated under the following principles. a) *Spectrum continuity:* Without spectrum conversion in this work, each link is assigned with the same FSs along the path. b) *Spectrum contiguity:* The FSs to be assigned should be continuous for each fiber link. c) *Spectrum conflict:* The spectrum allocation for each backup path is dedicated in CDP.

IV. JOINT ILP FORMULATION

In this section, we first give the sets, parameters, and variables of ILP. Then, we formulate a joint ILP model for CDP.

A. Sets, Parameters and Variables

For the sake of readability, we use $[|\mathbf{k}_r|]$, $\forall k$, $\forall b$, $\forall v$, $\forall a$, $\forall d$, $\forall c$, $\forall z$, $\forall m$, and $\forall r$ to denote $\{1, 2, \cdots, |\mathbf{k}_r|\}$, $\forall k \in [|\mathbf{k}_r|]$, $\forall b \in B$, $\forall v \in V$, $\forall a \in A$, $\forall d \in D$, $\forall c \in C$, $\forall z \in Z$, $\forall m \in M$, and $\forall r \in R$, respectively. We also use $\forall r \neq r'$, and $\forall k \neq k'$ to denote $\forall r, r' \in R, r \neq r'$, and $\forall k, k' \in [|\mathbf{k}_r|], k \neq k'$, respectively, if not indicated specifically.

The network sets and parameters are presented as follows.

- $G(V, A, D)$: Network with node set V, link set A and DC set D.
- C: Set of content.
- K: Number of assigned DCs for each content.
- R: Set of requests $r(s_r, z_r, |\mathbf{k}_r|, c_r, \phi_r)$, where s_r, z_r, $|\mathbf{k}_r|$, c_r and ϕ_r are source node, disaster zone that source node is placed, the number of paths that can be generated, content, and the the required number of FSs using BPSK, respectively. $|R|$ is the number of the requests.
- $\mathbf{k}_r$: Set of paths for the request r. $|\mathbf{k}_r|$ is the number of paths that can be generated. We use nodal degree of the source node to initialize $|\mathbf{k}_r|$. Note that we define the first path as the working path, and the last ($|\mathbf{k}_r|$-th) path as the backup path. For the second to $|\mathbf{k}_r| - 1$-th path, they are adaptively generated to minimize the spectrum utilization.
- D_r: Set of the content-placed DCs for request r. $|D_r|$ is the number of the content-placed DCs for request r.
- $m \in M$: The available modulation level set, *i.e.*, BPSK, QPSK, 8-QAM, and 16-QAM.
- h_m: Maximum transmission reach at modulation level m, which is $9,600$, $4,800$, $2,400$, and $1,200$, in km for BPSK, QPSK, 8-QAM, and 16-QAM, respectively [39]. h_{max}=9600 km.
- T_m: The spectrum efficiency. The available transmission rate per FS (12.5 GHz) for BPSK, QPSK, 8-QAM, and 16-QAM is 12.5, 25, 37.5, and 50, in $Gbps$, respectively. Thus, T_m is 1, 2, 3, and 4, respectively.
- d_a: The distance of link a in km.
- $k^{max}_{r,c}$: The maximum of $|\mathbf{k}_r|$ among the requests that require the content c.
- $z \in Z$: DZ/DZs set. $Z \subset G$ contains the sets of links and nodes.
- S: Set of FSs on each link. $|S|$ denotes the number of available FSs. The available bandwidth for One FS is 12.5 GHz in this work.
- ν^k_r: Configuration consisting of k working paths and a backup path to serve the request r.
- $\mu^k_{r,d}$: Generated path k from d to s_r.
- Ψ^+_v/Ψ^-_v: Set of outgoing/incoming links for node $v \in V$.

The Variables in ILP models for CDP are presented as follows.

- $p^k_{ra} \in \{0, 1\}$: Equals 1 if link a is used by the path k for request r.
- $\Lambda^k_{rd} \in \{0, 1\}$: Equals 1 if DC d is used as the end node of path k for request r.
- $\alpha^k_{rz} \in \{0, 1\}$: Equals 1 if the path k of r goes through DZ z.
- $R^{c_r}_d \in \{0, 1\}$: Equals 1 if content c, which is required by request r, is placed at DC d.
- $\Phi^k_{rm} \in [0, |S|]$: The number of FSs served for working/backup path w/B of request r with modulation format m.
- $w^k_r \in \{0, 1\}$: Equals 1 if the k-th path is used for request r. w^1_r and $w^{|\mathbf{k}_r|}_r$ equal 1, as they are chosen as the first working path, and backup path, respectively.
- $\xi^i_r \in \{0, 1\}$: Equals 1 if the number of working paths is i for request r, where the integer $i \in [|\mathbf{k}_r| - 1]$.
- $\Phi^k_{ra} \in [0, |s|]$: Integer variable denoting the assigned FSs on arc a for the k-th path of the request r.
- $g^k_r \in [0, |S| - 1]$: Integer variable denoting the assigned starting FS index of working path k for request r.
- $\beta^{kk'}_r \in \{0, 1\}$: Equals 1 if g^k_r is smaller than $g^{k'}_r$ for request r.
- $\beta^{kk'}_{rr'} \in \{0, 1\}$: Equals 1 if g^k_r of request r is smaller than $g^{k'}_{r'}$ of request r'.
- $\gamma^{kk'}_r \in \{0, 1\}$: Equals 1 if two working paths of the same request r have any common link.
- $\gamma^{kk'}_{rr'} \in \{0, 1\}$: Equals 1 if two working paths, k of r and k' of r', have any common link.
- $\Delta \in [0, |S|]$: Maximal index of the occupied FSs.

B. ILP Formulations

The studied disaster protection problem can be formulated by the following ILP, namely **CDP ILP**

$$\min \quad \theta_1 \cdot \sum_{a \in A} \sum_{r \in R} \sum_{k \in [|\mathbf{k}_r|]} \Phi^k_{ra} + \theta_2 \cdot \Delta \tag{1}$$

s.t. Constraints (2)-(30).

In the objective function, the first term calculates the total spectrum usage on all the links of all the paths, and the second term denotes the MOFI. Each link may exist FS fragments between any two assigned continuous FSs due to the spectrum continuity and spectrum contiguity. The MOFI, *i.e.* maximal occupied FS index, measures the load balancing of a network. In a healthy network, the MOFI of each link should be as even and small as possible. An un-balanced distributed MOFI would make the network at risk of node and link congestion under small traffics, and thus lower the transmission capacity of this network. In the rest of this work, we also use spectrum utilization referring to the objective. θ_1 and θ_2 are two adjustable weights. The constraints for CDP ILP can be divided into four parts, **DC assignment and content placement constraints** (2)-(4), **flow-conservation constraints** (5), **disaster-zone-disjoint path constraints** (6)-(8), **modulation adaption constraints** (9)-(12), **adaptive multi-path routing constraints** (13)-(21), and **spectrum allocation constraints** (22)-(30).

1) **DC assignment and content placement constraints**:

$$\sum_{d \in D} \Lambda^k_{rd} = w^k_r, \qquad \forall k, \forall r \tag{2}$$

Constraints (2) guarantee each DC can only be assigned for the working/backup path for once.

$$2 \leq \sum_{d \in D} R_d^{c_r} \leq |\mathbf{k}_r|, \qquad \forall r \tag{3}$$

Constraints (3) give the lower and upper bounds on the number of content storage DCs.

$$\sum_{k \in \mathbf{k}_r} \Lambda_{rd}^k \leq R_d^{c_r}, \qquad \forall r, \forall d \tag{4}$$

Constraints (4) assure that these DCs are different from each other so that the DZ-disjoint paths can be generated.

2) **Flow-conservation constraints**:

$$\sum_{a \in \Psi_v^+} p_{ra}^k - \sum_{a \in \Psi_v^-} p_{ra}^k = \begin{cases} w_r^k, & v = s_r \\ -\Lambda_{rv}^k, & v \in D, \\ 0, & \text{otherwise} \end{cases} \qquad \forall r, \forall k \tag{5}$$

Constraints (5) generate working paths and backup path through flow conservation. Specifically, the outgoing flow and incoming flow are equal for each content fragment, unless it is a destination (DC) node, which has an only incoming flow, or requesting node, which has only outgoing flow.

3) **Disaster-zone-disjoint path constraints**:

$$\alpha_{rz}^k \leq \sum_{a \in z} p_{ra}^k, \qquad \forall r, \forall z, \forall k \tag{6}$$

$$\alpha_{rz}^k \geq p_{ra}^k, \qquad \forall r, \forall z, \forall a \in z, \forall k \tag{7}$$

Constraints (6)-(7) determine whether the working paths and backup paths are affected by each DZ. Specifically, α_{rz}^k equals 1 if any path using any link(s) is affected by DZ z.

$$\sum_{k \in \mathbf{k}_r} \alpha_{rz}^k \leq 1, \qquad \forall r, \forall k, \forall z \in \{x | x \in Z, x \notin z_r\} \tag{8}$$

Constraints (8) ensure that the working and backup paths of the same request are generated as DZ-disjoint (except z_r). Note that the failure of z_r would absolutely block the requests with s_r. In this case, the request will be removed from our input request list directly, since it results in no protection solution.

4) **Modulation adaption constraints**

$$\sum_{a \in A} d_a \cdot p_{ra}^k \leq h_m + h_{max} \cdot (1 - b_{mr}^k), \qquad \forall r, \forall m, \forall k \tag{9}$$

$$\sum_{m \in M} b_{mr}^k \leq w_r^k, \qquad \forall r, \forall k \tag{10}$$

$$\Phi_r^k = \sum_{m \in M} \Phi_{mr}^k, \qquad \forall r, \forall k \tag{11}$$

$$\Phi_{mr}^k \leq b_{mr}^k \cdot |S|, \qquad \forall r, \forall k \forall m \tag{12}$$

Constraints (9) guarantee that the modulation format is selected with the maximum transmission reach for each path. Note that the path longer than h_{max} cannot be generated. Constraints (10) ensure that only one modulation format can be assigned for each path. Constraints (11) give the FS assigned for each request. Constraints (12) guarantee that no FS is assigned for the non-selected paths or none-selected modulation formats.

5) **Adaptive multi-path routing constraints**

$$p_{ra}^k \leq w_r^k, \qquad \forall r, \forall a, \forall k \tag{13}$$

$$\sum_{i=1}^{|\mathbf{k}_r|-1} w_r^i = \sum_{i=1}^{|\mathbf{k}_r|-1} i \cdot \xi_r^i, \qquad \forall r \tag{14}$$

$$\sum_{i=1}^{|\mathbf{k}_r|-1} \xi_r^i = 1, \qquad \forall r \tag{15}$$

$$w_r^1 = w_r^{|\mathbf{k}_r|} = 1, \qquad \forall r \tag{16}$$

$$w_r^k \geq w_r^{k+1}, \qquad \forall r, \forall k \in [|\mathbf{k}_r| - 2] \tag{17}$$

Constraints (13) prohibit the path generation if the k-th path is not selected. Constraints (14) and (15) indicate the number of working paths for the request. Constraints (16) assign the first path as the working path, and the last path as the backup path. Constraints (17) ensure that the paths with less index are to be preferred.

$$\sum_{m \in M} \Phi_{rm}^k \cdot T_m + (1 - w_r^k) \cdot \phi_r \geq \phi_r \cdot \sum_{i \in [|\mathbf{k}_r|-1]} \frac{\xi_r^i}{i}, \quad \forall r, \forall k \tag{18}$$

Constraints (18) ensure that the total FSs assigned on the working/backup paths are sufficient to serve the request, in which each path carries the same transmission rates for the request r.

$$\Phi_{ra}^k \leq p_{ra}^k \cdot |S|, \qquad \forall r, \forall k, \forall a \tag{19}$$

$$\Phi_{ra}^k \leq \Phi_r^k, \qquad \forall r, \forall k \tag{20}$$

$$\Phi_{ra}^k \geq \Phi_r^k - |S| \cdot (1 - p_{ra}^k), \qquad \forall r, \forall k, \forall a \tag{21}$$

Constraints (19)-(21) calculate the total FS on each link for each request.

6) **Spectrum allocation constraints**:

$$p_{ra}^k + p_{ra}^{k'} - 1 \leq \gamma_r^{kk'}, \quad \forall r, \forall a, \forall k, k', k > k' \tag{22}$$

$$\gamma_r^{kk'} = \gamma_r^{k'k}, \qquad \forall r, \forall k, k', k > k' \tag{23}$$

$$p_{ra}^k + p_{r'a}^{k'} - 1 \leq \gamma_{rr'}^{kk'}, \quad \forall r > r', \forall a, \forall k, \forall k' \in \mathbf{k}_{r'} \tag{24}$$

$$\gamma_{rr'}^{kk'} = \gamma_{r'r}^{k'k}, \qquad \forall r > r', \forall k \in \mathbf{k}_r, \forall k' \in \mathbf{k}_{r'} \tag{25}$$

Constraints (22)-(25) indicate whether any two paths have any common link.

$$\beta_r^{kk'} + \beta_r^{k'k} = 1, \qquad \forall r, \forall k, k', k > k' \tag{26}$$

$$\beta_{rr'}^{kk'} + \beta_{r'r}^{k'k} = 1, \qquad \forall r > r', \forall k \in \mathbf{k}_r, \forall k' \in \mathbf{k}_{r'} \tag{27}$$

Constraints (26) and (27)) compare the starting index of FSs between any two paths.

$$g_r^k + \Phi_r^k \leq \Delta, \qquad \forall r, \forall k \tag{28}$$

Constraints (28) imply the maximum index of occupied FSs.

$$g_r^k + \Phi_r^k - g_r^{k'} \le \Delta \cdot (2 - \gamma_r^{kk'} - \beta_r^{kk'}), \quad \forall r, \forall k, k', k \ne k' \tag{29}$$

$$g_r^k + \Phi_r^k - g_{r'}^{k'} \le \Delta \cdot (2 - \gamma_{rr'}^{kk'} - \beta_{rr'}^{kk'}), \quad \forall r, r', r \ne r', \forall k \in \mathbf{k}_r, \forall k' \in \mathbf{k}_{r'} \tag{30}$$

The spectrum conflict occurs if any two paths have any common link. Then based on the Starting Slot Assignment principle, which assigns the starting FSs to the demand, constraints (29) avoid spectrum conflict among the paths of the same request, and constraints (30) avoid spectrum conflict among the paths of different requests. The $spectrum\ contiguity$ is ensured by setting a contiguous range of FSs and for each path.

C. Computational Complexity

The number of dominant variables and constraints in CDP are $\max\{O(|R| \cdot |C| \cdot |D|, |R| \cdot |K| \cdot |Z|, |R| \cdot |K| \cdot |M|, |R| \cdot |K| \cdot |A|, |R|^2 \cdot |K|)\}$ and $\max\{O(|R| \cdot |C| \cdot |D|, |R| \cdot |K| \cdot |Z|, |R| \cdot |K| \cdot |M|, |R| \cdot |K| \cdot |A|, |R|^2 \cdot |K|)\}$, respectively.

V. Heuristics for CDP and M-CDP

To improve the scalability in the scenarios with large requests, we propose a heuristic algorithm to solve the adaptive path generation, and spectrum allocation. We then design a backtracking method to optimize the objective by minimizing the cost of each request path by path, forming the heuristic algorithm called heuristic for CDP (HCDP). Furthermore, we notice that the content storage space is of minimum if the number of paths is set as its maximum. Thus, we propose another maximum-CDP, namely M-CDP, to further reduce the content storage space. Note that if not indicated specifically, all the variables in this part are consistent with the Section IV.

A. Heuristic for CDP

We notice that the system performance is related to the number of paths, the number of hops for each path, the distance of each path, as well as the required spectrum resource. This is because the different number of paths leads to different overhead, which is caused by the rounding up of the spectrum resource division. Also, the number of hops for each request may increase dramatically as the number of paths grows, and it would require much more FSs in total. Thus, the number of paths is not the more the better. There may exist an optimal number of paths for each request in the given topology. To this end, we then propose an adaptive method to generate the paths for each request, in which all the possible paths combination would be taken into consideration. Accordingly, we propose the heuristic algorithm HCDP, whose pseudo-code is given in *Algorithm* 1.

The HCDP runs gives the pseudo-code of HCDP, which runs with the DC assignment and content placement obtained by using by ILP, *i.e.* ILP constraints (2)-(4), where constraints (2) are rewritten as

$$\sum_{d \in D} \Lambda_{rd}^k = 1, \qquad \forall k, \forall r \tag{31}$$

The objective is to minimize the overall hops from DCs to source nodes. *Algorithm* 1 uses three steps to solve the problem. At first, we generate the solution set request by request based on the given $\mathbf{k}_r$ and then select the initial solution with minimal cost of each request. It is a greedy algorithm, shown in *lines 2-22*. Next, we use a coloring algorithm to generate a conflict graph for all the paths based on the initial solution. Then we assign the spectrum usage based on the conflict graph, shown in *lines 23-25*. Finally, we backtrack the generated solution set to find whether there is a better solution with less total cost, shown in *lines 26-39*.

Line 1 initializes all the variables and sets. *Line 3* sets nodal degree as the upper bound of the number of paths. *Lines 5-6* update the network topology by removing the DZ-joint node(s) and link(s) of the former generated path, such that the next generated path is DZ-disjoint. *Lines 7-8* compute the shortest path from each DC with required content $c_r(d \in D_r)$ to the source node. *Lines 9-11* assign the modulation format for the path with as the higher transmission rate as possible. *Line 12* calculates the cost for each path. The cost of the path is the sum of spectrum usage, shown as

$$cost_p^r = (\sum_{a \in A} p_{ra}^k \cdot \Phi_r^k) \tag{32}$$

where p_{ra}^k equals 1 if link a is used by path k, and Φ_r^k is the number of FSs reserved for the k-th path of request r.

Lines 13-14 select the path with minimal cost as the working path for the request r and the corresponding DC d as the primary DC and put the path into the path set $\mathbf{k}_r$. *Lines 15-19* generate the paths as many as possible configurations for each request. We regard every succeeded generation with more than two paths as one candidate configuration since it can offer complete path protection. The value $k-1$ is the number of working paths of the configuration ν_r^k. Then, we calculate the cost of each configuration and select the best one with the optimal number of paths as the solution for the request. The cost for one configuration is computed by Eq. (33).

$$cost_{conf}^{r,\nu} = \sum_{k \in \nu_r^k} \sum_{a \in A} p_{ra}^k \cdot \Phi_r^k \tag{33}$$

where p_{ra}^k equals 1 if link a is used by k-th path of configuration ν_r^k, and ν_r^k is a configuration with $|k|$ generated paths for request r.

Lines 23-25 generate conflict graph to assign the FSs [29]. The conflict graph is generated based on a coloring algorithm, whose details can be referred to [29]. *Lines 26-27* calculate the total cost and find the link with the MOFI. Similarly, the total cost can be expressed in Eq. (34).

$$cost_{total} = \theta_1 \cdot (\sum_{a \in A} p_{ra} \cdot \Phi_r^k) + \theta_2 \cdot \Delta \tag{34}$$

Although it may achieve minimal spectrum usage for each request, it may not be the best solution for the entire network,

Algorithm 1: HCDP Algorithm

Input : $G(V, A, D)$, D_r, $R_d^{c_r}$, $\forall r$, $\forall z$, F_max, S.
Output: $\mu_{r,d}^k$, path list $\{\mathbf{k}_r | r \in R\}$, $cost_{total}$

1 Initialize all variables as zero ($\mu_{r,d}^k \leftarrow 0$, $\mathbf{k}_r \leftarrow \emptyset$);
2 **for** $r \in R$ **do**
3 $\quad \bar{k}_r \leftarrow$ nodal degree of s_r in G; $G^1 \leftarrow G$;
4 $\quad$ **for** $k \in [\bar{k}_r]$ **do**
5 $\quad\quad$ **if** $k > 1$ **then**
6 $\quad\quad\quad G^k \leftarrow G^{k-1} \setminus$ {the DZ-joint (except z_r) links and nodes in the path p_r^{k-1} ($\mu_{r,d}^{k-1} = 1$)};
7 $\quad\quad$ **for** $d \in D_r : R_d^{c_r} = 1, d \in G_k(\mu_{r,d}^{k-1} \neq 1)$ **do**
8 $\quad\quad\quad$ In G^k, if the shortest path from d to s_r (noted as $p_{r,d}^k$) can be found, then calculate its length $l_{r,d}^k$.
9 $\quad\quad\quad$ **for** $m \in M$ **if** $h_m < l_{r,d}^k \leq h_{m-1}$ **then**
10 $\quad\quad\quad\quad \bar{\Phi}_r^k \leftarrow \lceil \phi_r \,/\, T_{m-1} \rceil$;
11 $\quad\quad\quad$ **do**
12 $\quad\quad\quad\quad$ Calculate the cost of $p_{r,d}^k$ using Eq. (32);
13 $\quad\quad$ **if** *At least one path can be found* **then**
14 $\quad\quad\quad$ Select the path from d to s_r with the minimal cost as the k-th path (noted as p_r^k), $\mathbf{k}_r \leftarrow \mathbf{k}_r \cup \{p_r^k\}$, $\mu_{r,d}^k \leftarrow 1$;
15 $\quad\quad\quad$ **if** $k \geq 2$ **then**
16 $\quad\quad\quad\quad$ Generate a new candidate configuration ν_r^k;
17 $\quad\quad\quad\quad$ Set p_r^k as the backup path and the others in $\mathbf{k}_r$ as working paths;
18 $\quad\quad\quad\quad |\mathbf{k}_r| \leftarrow k$; $\forall k' \in [k], \Phi_r^{k'} \leftarrow \lceil \frac{\bar{\Phi}^{k'}_r}{k-1} \rceil$;
19 $\quad\quad\quad\quad$ Calculate the cost for the candidate configuration using Eq. (33);
20 $\quad\quad$ **else**
21 $\quad\quad\quad$ **Break**;
22 $\quad$ Select the candidate configuration with minimal cost for request r, and update $|\mathbf{k}_r|$ accordingly;
23 **for** $r \in R$ **do**
24 $\quad$ **for** k ***from*** 1 ***to*** $|\mathbf{k}_r|$ **do**
25 $\quad\quad$ Generate conflict graph, and allocate FSs based on the conflict graph [29];
26 Calculate the MOFI, $\Delta \leftarrow$ MOFI;
27 Calculate $cost_{total}$ using Eq. (34);
28 $L_{max} \leftarrow L_{max} \cup$ {link(s) with the MOFI};
29 **for** i ***from*** 1 ***to*** F_max **do**
30 $\quad$ **for** $r \in R$ **do**
31 $\quad\quad$ **for** $d \in D_r : \mu_{r,d}^k = 1$ **do**
32 $\quad\quad\quad$ **for** $a : p_{ra}^k = 1$ **do**
33 $\quad\quad\quad\quad$ **if** $a \in L_{max}$ **then**
34 $\quad\quad\quad\quad\quad G' \leftarrow G \setminus \{a\}$;
35 $\quad\quad\quad\quad\quad$ Regenerate all the possible solutions based on G';
36 $\quad\quad\quad\quad\quad$ **if** $\exists$ *solution with* $cost'_{total} < cost_{total}$ **then**
37 $\quad\quad\quad\quad\quad\quad cost_{total} \leftarrow cost'_{total}$;
38 $\quad\quad\quad\quad\quad\quad L_{max} \leftarrow L_{max} \setminus \{a\}$;
39 $\quad\quad\quad\quad\quad\quad L_{max} \leftarrow L_{max} \cup$ {link(s) with the MOFI};

especially for the MOFI. Also, it is of large probability that the selected configuration is at the same cost as other candidate configurations. Therefore, *Line 28* finds the link(s) of the MOFI. *Lines 29-39* give the descent method for total cost by regenerating the paths before it fails until a preset number of times. The regeneration principle is to avoid using the link(s) of the MOFI, such that the spectrum usage can remain the same and the MOFI would be reduced. Note that there exists a Ping-Pong effect, *e.g.*, the MOFI alternates to occur in a few specific links in every iteration, and yet the cost still remains the same. To avoid such a situation, we use F_max as the maximum failure times to limit the backtracking process.

In Algorithm 1, the computational complexity for the first step, *i.e. lines 2-22*, to generate initial solution and solution set is $O(|R| \cdot |D| \cdot |V| \cdot |M| \cdot \log |A|)$. The computational complexity for the spectrum usage assignment is $O(\log(|R| \cdot |K|))$ [29]. Thus, the computational complexity of the second step, *i.e. lines 23-25*, is $O(|R| \cdot |K| \cdot \log(|R| \cdot |K|))$. the computational complexity of the third step, *i.e. lines 26-39*, of backtracking is $O(\text{F\_max} \cdot |R| \cdot |D| \cdot |A| \cdot (|R| \cdot |D| \cdot |V| \cdot |M| \cdot \log |A| + |R| \cdot |K| \log(|R| \cdot |K|)))$, which is also the computational complexity for Algorithm 1.

B. Maximum-CDP

We notice that there exists a trade-off between content storage space and spectrum usage. For a content storage space of l, k working paths can reduce the content storage space on each DC to $\frac{l}{k}$. However, each additional path may also have more hops/links than the former one, then the FSs overhead on the additional path is more than reduced FSs on the backup path. As a consequence, the spectrum usage may not be optimal for M-CDP. Therefore, We design M-CDP to optimize content storage space, aiming to serve the requests with as many paths as possible.

To generate M-CDP, we can simply remove *lines 15-19* of Algorithm 1 and replace *line 22* with:

- Set p_r^k as the backup path and the others in $\mathbf{k}_r$ as working paths; $\Phi_r^{k'} \leftarrow \lceil \frac{\bar{\Phi}^{k'}_r}{|\mathbf{k}_r|-1} \rceil$;Calculate the cost for the candidate configuration using Eq. (33);

VI. Simulations and Performance Evaluations

In this section, extensive simulations have been done to assert the performance of the proposed CSS-based CDP protection schemes. we first compare the system performance between CDP and DP, using ILP for small-scale requests. Then, we study the efficiency of the HCDP and its gap to the optimal solution computed by the ILP model. Next, for a large scale of requests, we evaluate the system performance by using the heuristic algorithm proposed for DP and different CDP schemes respectively. The simulations are conducted for the different number of available DC locations and number of replicas per content, *i.e.* K. The M-CDP with as many as possible $|\mathbf{k}_r|$ is also validated. At last, to assert the performance of storage space, we assume the total size of the original content data is normalized as 1. We assume the content is first divided into 10 parts, and then encoded to at most $10 \times K$

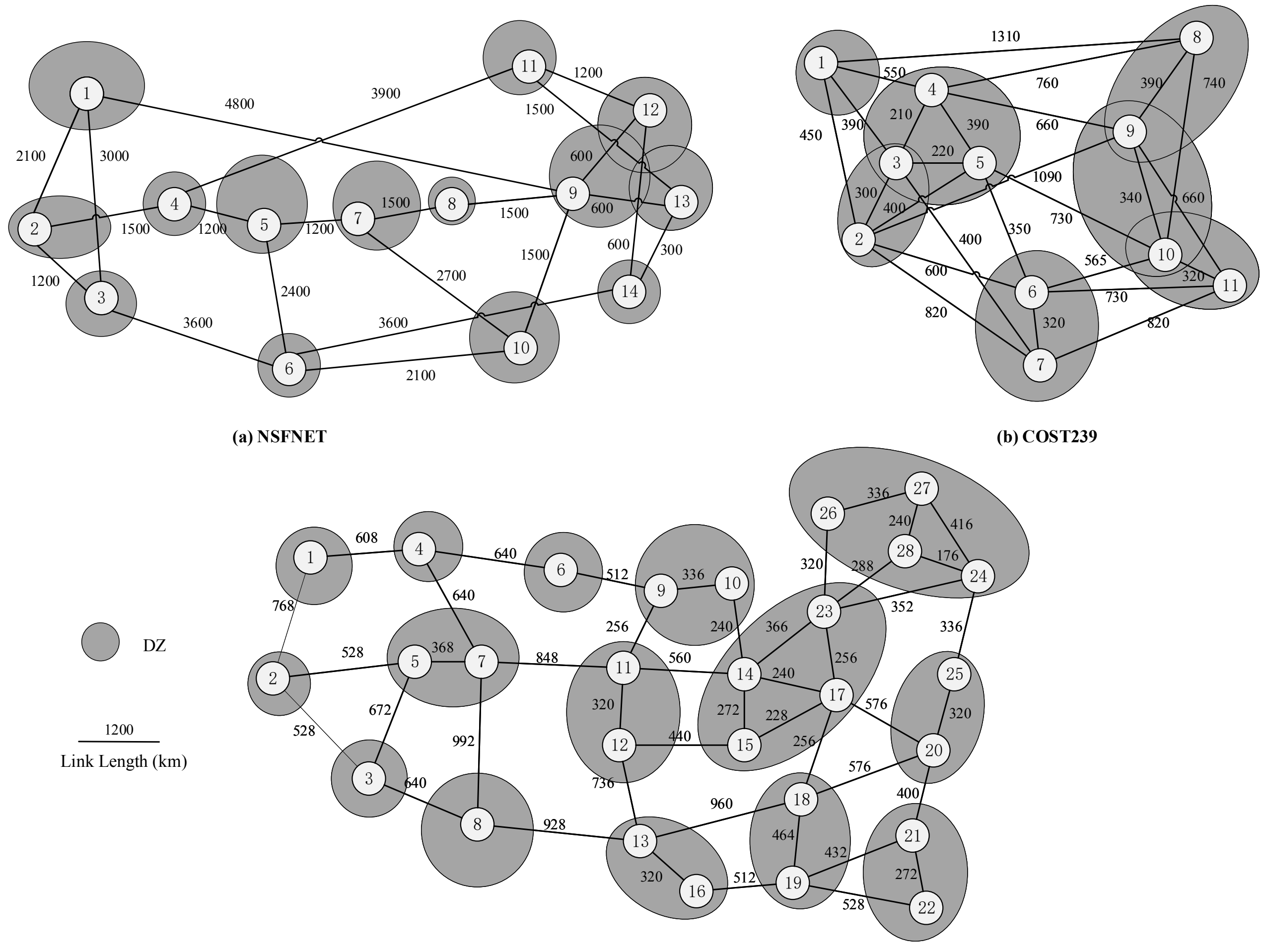

(a) NSFNET

(b) COST239

(c) US Backbone network

Fig. 2. Topology of the testbeds used in simulations.

fragments via a rateless coding [41], where K is the number of assigned DCs per content. Note that the overall content storage space depends on the results of CDP, and $10 \times K$ fragments is the upper bound of the content storage space. Thus, in the traditional mirrored storage system, the storage space for each content equals K.

A. Simulation settings

We use CPLEX 12.60 to solve the proposed ILP model and heuristic on a PC with a 3.6 GHz CPU and a 64 GBytes RAM. In order to fairly evaluate the pros, cons, and applicable scenarios of CDP, we make the following comparisons in three classical EO-DCN testbeds NSFNET (14 nodes, 44 directed links, 14 DZs, average link length 1936 km, and average nodal degree 3.14), COST239 (11 nodes, 52 directed links, 7 DZs, average link length 578 km, and average nodal degree 4.73), and US Backbone network (28 nodes, 90 directed links, 15 DZs, average link length 466 km, and average nodal degree 3.2):

- Efficiency of the HCDP compared with the ILP model, with 3 DCs at 5 available DC locations;
- Optimal spectrum efficiency utilization of CDP and DP (**computed by solving the proposed ILP model**) with small scale of requests, with 3 DCs at 5 available DC locations;
- Spectrum efficiency utilization of CDP, DP, and M-CDP (**computed by using the proposed heuristic algorithms**) for large scale of requests , when varying the number of available DC locations, *i.e.* $|D|$, and the number of DCs per content, *i.e.* K;
- Content storage space for different CDP, DP, and M-CDP;
- Analysis on weights using ILP with 5 DCs.

The topologies are shown in Fig. 2. It can be seen that NSFNET is a low-connected network, while COST-239 is a dense network with higher connectivity, and US Backbone network is even denser but with low connectivity. As disaster prediction is still a critical issue to be addressed, we adopt the disaster zones used in the previous studies [28] [2] [25], which are generated randomly with a range up to 170 km [42]. Each DZ involves the group of affected nodes and links. The simulation parameters for different scenarios are set as follows. In NSFNET: 1) 5 available DC locations at nodes 2, 5, 6, 9 and 11; 2) 4 available DC locations at nodes 2, 5, 9 and 11. In COST239: 1) 5 available DC locations at nodes 1, 2, 7, 8 and 11; 2) 4 available DC locations at nodes 1, 2, 7 and 8. In US Backbone network: 1) 8 available DC locations at nodes 1, 7,

TABLE II
QUALITY OF SOLUTION AND EXECUTION TIME IN JOINT ILP MODELS AND THE HCDP.

Method	Joint ILP model				HCDP				
Number of Requests	$Objective$	FS_{total}	$MOFI$	$Time(s)$	$Objective$	FS_{total}	$MOFI$	$Time(s)$	Gap
NSFNET Network, 3 DCs at available locations of nodes 2, 5, 6, 9, and 11									
10	**58**	52	6	34	**74**	69	5	4	**18.97%**
20	**117**	107	10	10800	**120**	113	7	17	**2.56%**
30	**190**	174	16	10800	**226**	212	14	32	**18.95%**
40	**-**	-	-	10800	**279**	266	17	57	**-**
COST239 Network, 3 DCs at available locations of nodes 1, 2, 7, 8, and 11									
10	**50**	45	5	10800	**51**	45	6	1	**2.00%**
20	**96**	85	10	10800	**88**	80	8	6	**-8.33%**
30	**149**	133	16	10800	**137**	124	13	13	**-8.05%**
40	**-**	-	-	10800	**199**	165	21	24	**-**

- No feasible ILP solution is obtained after 3 hours or exhausting all the memory.

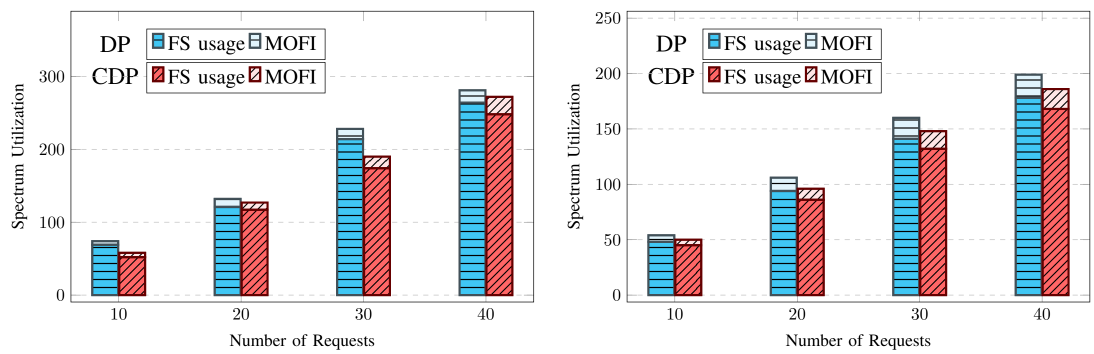

(a) Spectrum Utilization in NSFNET

(b) Spectrum Utilization in COST239

Fig. 3. Spectrum Utilization of DP and CDP using ILP in NSFNET, and COST239.

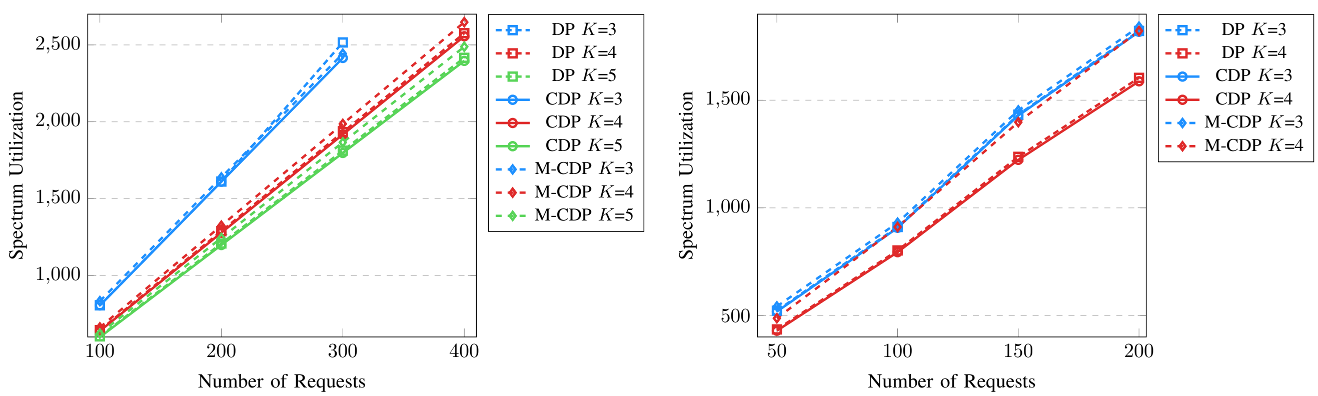

(a) Spectrum Utilization versus K (in 5 available DC locations)

(b) Spectrum Utilization versus K (in 4 available DC locations)

Fig. 4. Spectrum Utilization versus number of available DC locations in NSFNET using HCDP.

9, 12, 14, 19, 21 and 28; 2) 6 available DC locations at nodes 1, 7, 14, 19, 21 and 28. These DC locations are randomly chosen. Then, to evaluate the disaster resilience performance of EO-DCNs with CSS, we compare different CDPs with DP [28] [2]. We consider the static scenarios, where the requests are randomly generated with 10 contents, and the required transmission rate is randomly generated following uniform distribution among $(0, 125\,Gbps]$. Each link is set with a maximum of 300 FSs to carry the traffic. For simplicity, the weights of the objective, *i.e.* the weighted sum of spectrum usage and MOFI, are set as the same value, *i.e.* $\theta_1 = \theta_2 = 1$, except in the subsection *Analysis on Weight*. To ease the readability, we use spectrum utilization in the simulations to refer to the objective aforementioned. We also set F_max as 100 in the HCDP.

B. Validation of Efficiency of the HCDP Compared with ILP

To verify the efficiency of the HCDP, we conduct simulations under small traffic demands (the number of requests varies from 10 to 40) with both the ILP model and the HCDP

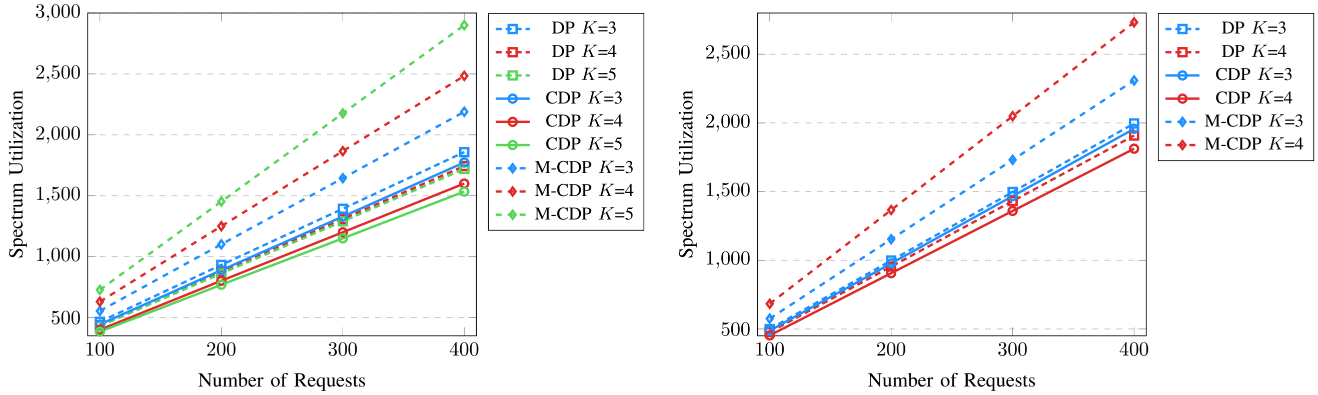

(a) Spectrum Utilization versus K (in 5 available DC locations)

(b) Spectrum Utilization versus K (in 4 available DC locations)

Fig. 5. Spectrum Utilization versus number of available DC locations in COST239 using HCDP.

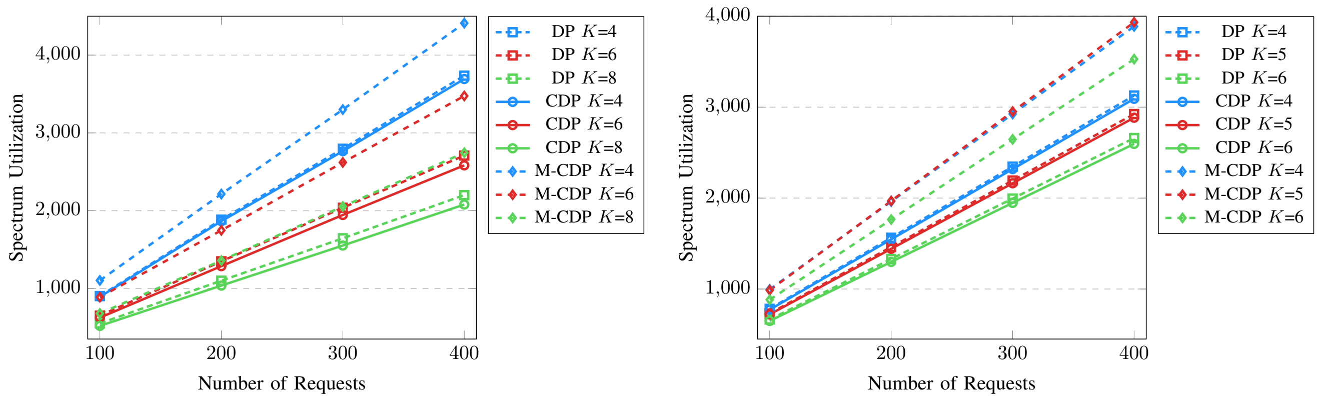

(a) Spectrum Utilization versus K (in 8 available DC locations)

(b) Spectrum Utilization versus K (in 6 available DC locations)

Fig. 6. Spectrum Utilization versus number of available DC locations in US Backbone network using HCDP.

in NSFNET and COST239 networks, while the execution time is limited to $10800s$. The results are summarized in Table II. We assume that in the NSFNET network there are 3 DCs with 5 available locations (at nodes 2, 5, 6, 9, and 11) per content, and in the COST239 network, there are 3 DCs with 5 available locations (at nodes 1, 2, 7, 8 and 11) per content.

Table II elucidates the solution of total spectrum utilization ($Objective$ in the table) and computation time of ILP and HCDP. Due to the high computational complexity, the joint ILP model requires in total $10800s$ for more than 20 requests in the NSFNET network, while that is 10 in the COST239 network. The ILP model cannot solve the problem once the number of requests scales 40 after $10800s$. It can be seen that the execution time in the HCDP is negligible. However, the introduced gap is a bit high in the NSFNET for the HCDP at 10, because the DC assignment and content placement are pre-determined and solved separately. For a low-connected network, the DC assignment and content placement severely impact the spectrum utilization. However, it can also be noticed that the solution of the HCDP is much closer to that of the ILP in the COST239 network. As the number of requests increases to more than 10, ILP cannot solve the problem to optimality, let alone to get a near-optimal solution. The computation is more complicated in a dense and high-connected network. Thus, the performance of HCDP is even better than that of ILP.

C. Validation of CDP Compared with DP for Small-Scale Instances (Using ILP)

Let us then investigate the spectrum utilization of CDP compared with DP for small-scale instances (the number of requests varies from 10 to 40). We assume that 3 DCs with 5 available locations (at nodes 2, 5, 6, 9, and 11) per content in the NSFNET network, and 3 DCs with 5 available locations (at nodes 1, 2, 7, 8, and 11) per content in the COST239 network. As shown in Fig. 3(a) and Fig. 3(b), performances of the CDP scheme are better than the traditional schemes, the spectrum utilization is improved. The reduction of spectrum utilization is up to 21.6% in NSFNET. Such improvement is because the proposed CDP scheme allows the multiple DZ-disjoint working paths generation, and FSs allocated for the backup path to protect one working path are reduced at least by half. The reduction of spectrum utilization in the COST239 network for CDP can also be observed. Note that in some cases, the MOFI is worse for the CDP. Compared to the DP, the CDP allows less FS usage for each request by sharing the traffic on multiple paths. However, sometimes it will cause the over utilization of the links adjacent to DCs. Consequently, the

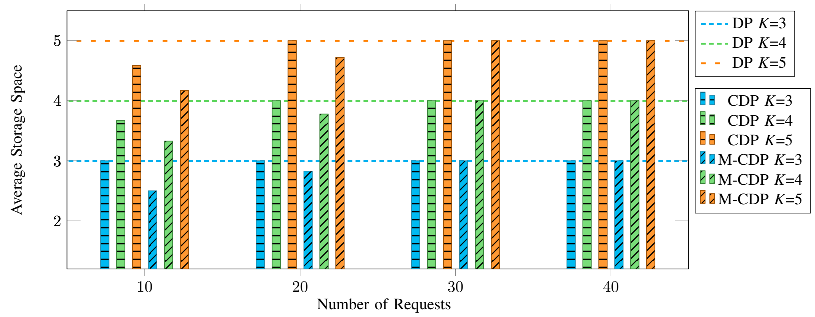

(a) Average Storage Space per Content in NSFNET

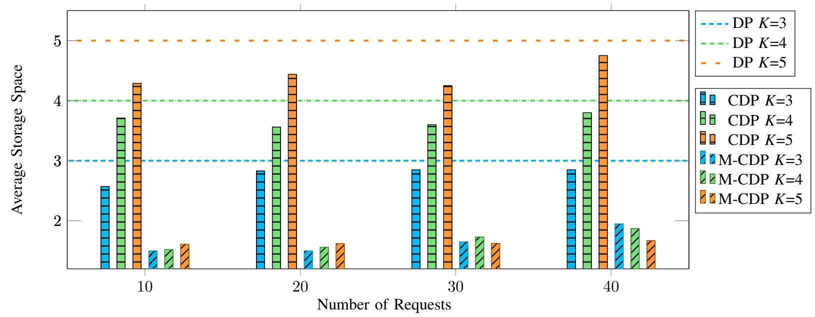

(b) Average Storage Space per Content in COST239

Fig. 7. Storage Space Performance for 5 available DC locations per Content.

MOFI on these links may be higher for CDP when the number of requests varies from 10 to 40. Even with the cons, the CDP still chooses the solution with multiple working paths, because the overall spectrum utilization is less, as shown in Fig. 3(a).

D. Validation of CDPs Compared with DP for Large-scale Instances (Using HCDP)

To further explore the performance of CDP, we use heuristics to evaluate DP, CDPs, and M-CDP on the situation with a large scale of requests in the networks of NSFNET, COST239, and US Backbone network, where the number of requests is up to 400. The scenarios are with the different number of available DC locations and K. Note that the number of requests is from 50 to 200 in Fig. 4(b), because the required bandwidth beyond the maximum transmission capacity in some links under this scenario, when the number of requests is more than 200. Due to the same reason, some points cannot be generated in Fig. 4(a), *i.e.* $K = 3$ and number of requests is 400. Note that the US Backbone network is a much denser network with a shorter average link distance compared to NSFNET and COST239. Also, with more available DCs, the requests are provisioned with shorter path lengths, thus with higher modulation formats. Therefore, the number of the provisioned requests can reach 400. However, the total spectrum utilization for all links is much higher since the number of links is larger compared to other networks.

As shown in Fig. 4(a) and 4(b), compared with DP, the performance improvement of CDP is small in NSFNET, because in such a low-connected network, the number of paths that can be generated for most nodes is no larger than 2, and the principle on disaster resilience also exacerbates this issue. These results that most requests are provisioned with one working path and one backup path. Thus, the solutions of CDP and DP tend to be the same, as well as the spectrum utilization. However, the performances are quite different in COST239 network, as demonstrated in Fig. 5(a) and 5(b). This is because the connectivity of the COST239 network is high enough to support multi-path routing, where the number of the paths is up to 5. As a consequence, CDP outperforms the others, since adaptive multi-path routing elucidates its superiority. Similar significant improvement can also be observed in the US Backbone network, whose results are plotted in Fig. 6(a) and 6(b). The biggest reduction is obtained with large K and 8 available DC locations. With more DCs, it becomes easier for the CDP to find more appropriate DCs locations for each request, which can significantly promote the quality of the generated routing paths to reduce the spectrum usage. While reducing the number of DCs will degrade the quality of the generated routing paths. Therefore, we can conclude that the advantages of the CDP are more evident in the high-connected networks with more available DCs. However, M-CDP is worse than DP in these scenarios. The reason is that the number of paths is too large, and the cost for the 4-th or 5-th path is much larger than the formerly generated paths for having more routing hops. Thus, the extra cost is bigger than the reduced spectrum resource reserved on the backup path. A trade-off between the number of paths and spectrum utilization can be observed. We will discuss it in the next subsection. The improved spectrum utilization is at most from $K = 3$ to $K = 4$ in Fig. 4(a). We also notice that the spectrum utilization of the same K is better with more DC locations, in both NSFNET and COST239. It demonstrates the DC locations also have a significant impact on the system performance.

TABLE III
OBJECTIVE OF CDP VERSUS DIFFERENT WEIGHTS WITH 20 REQUESTS (USING ILP).

Weights Ratio ($\theta_1 : \theta_2$)	0:1	0.1:1	0.5:1	1:1	1:0.5	1:0
NSFNET Network, 5 DCs at nodes 2, 5, 6, 9, and 11						
Objective	10	20.2	61	112	108	102
FS_{total}	119	102	102	102	102	102
MOFI	10	10	10	10	10	300
COST239 Network, 5 DCs at nodes 1, 2, 7, 8, and 11						
Objective	6	15.6	53	98	94	90
FS_{total}	196	96	90	90	90	90
MOFI	6	6	8	8	8	300

E. Analysis on Content Storage Space

We then give the content storage space performance based on all DP, CDP, and M-CDP varying different number of DCs with 5 available locations of nodes 2, 5, 6, 9, and 11 in NSFNET, and at nodes 1, 2, 7, 8 and 11 in the COST239 network, respectively. In Fig. 7 (a) and (b), CDP also elucidates the superiority on storage space, and the storage space is cut up to 50%, especially in the COST239 network. With the normalized storage space, the average storage space per content for a traditional storage system is K, *i.e.* number of DCs. For the CSS, it only depends on the potential source nodes. Besides, the scenario with a small scale of requests can be seen as the targeted content provisioning applications, in which the content is only supplied for a small part of the nodes in the network due to the concerns of copyright, cost, etc. Thus, the proposed systems achieve lower storage space in such a scenario. As request number increases in the NSFNET network, the even distribution of requests tends to traverse all network nodes, and consequently, storage space will grow to serve the request with $|\mathbf{k}_r| = 2$, *i.e.* only two paths can be generated due to disaster resilience consideration. Therefore, the storage space of the CSS tends to have the same storage space as the conventional one in Fig. 7 (a). However, the nodal degree in the COST239 network is large enough, in which the minimum $|\mathbf{k}_r|$ is 3. Thus, the CDP in such a situation allows a storage space reduction up to 14%, and its improvement keeps existing as the number of requests increases. Furthermore, M-CDP achieves the least storage space with a reduction up to 67.8%, because more working paths allow less spectrum resource split for each path and less storage space needs for each DC. Hence, M-CDP with larger $|\mathbf{k}_r|$ can cut more content storage space. However, as discussed in the last subsection, the decrement of the content storage space in M-CDP comes with the price of high spectrum resources, while CDP nicely balances the spectrum utilization with substantial storage space saving.

F. Analysis on Weights

We now investigate the impact of different weights, *i.e.*, θ_1 and θ_2, in the situation with 20 requests using ILP. The parameters of the networks are set with 5 DCs at nodes 2, 5, 6, 9, and 11 in the NSFNET network, and at nodes 1, 2, 7, 8, and 11 in the COST239 network, respectively. θ_1 weights the overall FSs usage (FS_{total}), and θ_2 weights the MOFI. Considering FSs usage is usually dozens of times of MOFI, we then change the ratio of θ_1 and θ_2 varies $0 : 1$, $0.1 : 1$, $0.5 : 1$, $1 : 1$, $1 : 0.5$, and $1 : 0$, and calculate the objective, FS usage, and MOFI of these solutions, to explore the performances under different weightings. As shown in Table III, we can see that the optimizations of single-objective, *i.e.* $\theta_1 = 0$ and $\theta_2 = 0$, cause either high MOFI or high FS usage in both topologies. Note that for $\theta_2 = 0$, the MOFI is of the maximum of the link capacity, *i.e.* 300 FSs. Because it is not optimized in the objective function. For the joint optimization, although the objectives are different, the FS usage and MOFI remain the same value for rest weights combinations in NSFNET. It shows the obtained solutions do not differ from each other, because the available routes from the source node to the assigned DC are few in such a sparse network, and it is easy to get the optimal solution for the combination of each weight. Thus, these solutions tend to get the same output. While in COST239 network, as $\theta_1 : \theta_2$ increases from $0.1 : 1$ to $0.5 : 1$, the FSs usage decreases and MOFI increases. Then the solutions remain the same for other weight ratios. Such a change is consistent with the weights change.

VII. CONCLUSION

In this paper, we proposed a novel disaster protection scheme in EO-DCNs leveraging CSS and adaptive multi-path routing. Our protection scheme proposes to guarantee 100% disaster resilience with near-optimal spectrum utilization and substantial content storage space saving for the first time, which allows service provisioning with adaptive multi-path routing. In CDP, each content is jointly encoded via rateless code, which is then distributed on no-less than three DCs located in different DZs. To jointly minimize the spectrum usage and MOFI, we formulated CDP as an ILP and also proposed a fast heuristic algorithm. To improve further the system performance of content storage space, we then develop M-CDP to generate a maximal number of working paths for each request. At last, we evaluated and analyzed CDP and M-CDP via simulations. Simulation results confirm that the proposed protection scheme CDP outperforms its counterpart by saving up to 21.6% spectrum utilization and 15% content storage space. CDP elucidates its superiority, especially in a densely connected network.

REFERENCES

[1] Y. Liu, F. Zhou, C. Chen, Z. Zhu, T. Shang, and J.-M. Torres-Moreno, "Disaster protection in Inter-DataCenter networks leveraging cooperative storage," in *in Proc. of IEEE Global Communications Conference (Globecom'20)*, Taipei, Taiwan, Dec. 2020.

[2] M. Ju, F. Zhou, and S. Xiao, "Disaster-resilient cloud services provisioning in elastic optical inter-data center networks," in *Proc. IEEE Int. Symp. on Model., Anal., and Simul. of Comput. and Telecommun. Syst. (MASCOTS)*, Oct. 2019, pp. 116–124.

[3] Z. Zhu, W. Lu, L. Zhang, and N. Ansari, "Dynamic service provisioning in elastic optical networks with hybrid single-/multi-path routing," *J. Lightw. Technol.*, vol. 31, pp. 15–22, Jan. 2013.

[4] L. Gong, X. Zhou, X. Liu, W. Zhao, W. Lu, and Z. Zhu, "Efficient resource allocation for all-optical multicasting over spectrum-sliced elastic optical networks," *J. Opt. Commun. Netw.*, vol. 5, pp. 836–847, Aug. 2013.

[5] M. F. Bari, R. Boutaba, R. Esteves, L. Z. Granville, M. Podlesny, M. G. Rabbani, Q. Zhang, and M. F. Zhani, "Data center network virtualization: A survey," *IEEE Commun. Surveys Tut.*, vol. 15, no. 2, pp. 909–928, Apr. 2013.

[6] M. F. Habib, M. Tornatore, F. Dikbiyik, and B. Mukherjee, "Disaster survivability in optical communication networks," *Comput. Commun.*, vol. 36, no. 6, pp. 630–644, 2013.

[7] B. Wang, Z. Qi, R. Ma, A. Vasilakos, and H. Guan, "A survey on data center networking for cloud computing," *Comput. Netw.*, vol. 91, p. 528–547, Sep. 2015.

[8] F. Zhou, J. Liu, G. Simon, and R. Boutaba, "Joint optimization for the delivery of multiple video channels in telco-cdns," *IEEE Transactions on Network and Service Management*, vol. 12, no. 1, pp. 87–100, 2015.

[9] S. Neelam and S. K. Sood, "A scientometric review of global research on smart disaster management," *IEEE Transactions on Engineering Management*, vol. 68, no. 1, pp. 317–329, 2021.

[10] "How effective is your data center's disaster recovery plan?" [Online]. Available: http://www.lifelinedatacenters.com/data-center/effective-disaster-recovery-plan/.

[11] L. Gong and Z. Zhu, "Virtual optical network embedding (VONE) over elastic optical networks," *J. Lightw. Technol.*, vol. 32, pp. 450–460, Feb. 2014.

[12] P. Lu, L. Zhang, X. Liu, J. Yao, and Z. Zhu, "Highly-efficient data migration and backup for big data applications in elastic optical inter-datacenter networks," *IEEE Netw.*, vol. 29, pp. 36–42, Sept./Oct. 2015.

[13] T. Gomes, J. Tapolcai, C. Esposito, D. Hutchison, F. Kuipers, J. Rak, A. de Sousa, A. Iossifides, R. Travanca, J. André, L. Jorge, L. Martins, P. O. Ugalde, A. Pašić, D. Pezaros, S. Jouet, S. Secci, and M. Tornatore, "A survey of strategies for communication networks to protect against large-scale natural disasters," in *Proc. Int. Workshop on Resilient Netw. Des. and Model. (RNDM)*, Sep. 2016, pp. 11–22.

[14] "Caict," [Online]. Available: http://www.caict.ac.cn/.

[15] "Synergy research," [Online]. Available: https://www.srgresearch.com/.

[16] A. G. Dimakis, P. B. Godfrey, Y. Wu, M. J. Wainwright, and K. Ramchandran, "Network coding for distributed storage systems," *IEEE Trans. on Info. Theory*, vol. 56, no. 9, pp. 4539–4551, Sep. 2010.

[17] J. Yao, P. Lu, L. Gong, and Z. Zhu, "On fast and coordinated data backup in geo-distributed optical inter-datacenter networks," *Journal of Lightwave Technology*, vol. 33, no. 14, pp. 3005–3015, 2015.

[18] X. Xie, Q. Ling, P. Lu, W. Xu, and Z. Zhu, "Evacuate before too late: Distributed backup in inter-dc networks with progressive disasters," *IEEE Transactions on Parallel and Distributed Systems*, vol. 29, no. 5, pp. 1058–1074, 2018.

[19] A. Agrawal, V. Bhatia, and S. Prakash, "Network and risk modeling for disaster survivability analysis of backbone optical communication networks," *J. Lightw. Technol.*, vol. 37, no. 10, pp. 2352–2362, May 2019.

[20] S. S. Savas, M. F. Habib, M. Tornatore, F. Dikbiyik, and B. Mukherjee, "Network adaptability to disaster disruptions by exploiting degraded-service tolerance," *IEEE Communications Magazine*, vol. 52, no. 12, pp. 58–65, 2014.

[21] C. Develder, J. Buysse, B. Dhoedt, and B. Jaumard, "Joint dimensioning of server and network infrastructure for resilient optical grids/clouds," *IEEE/ACM Trans. on Netw.*, vol. 22, no. 5, pp. 1591–1606, Oct. 2014.

[22] A. Pašić, R. Girão-Silva, B. Vass, T. Gomes, and P. Babarczi, "Fradir: A novel framework for disaster resilience," in *Proc. Int. Workshop on Resilient Netw. Des. and Model. (RNDM)*, Aug. 2018, pp. 1–7.

[23] L. Tomás, P. Kokkinos, V. Anagnostopoulos, O. Feder, D. Kyriazis, K. Meth, E. Varvarigos, and T. Varvarigou, "Disaster recovery layer for distributed openstack deployments," *IEEE Transactions on Cloud Computing*, vol. 8, no. 1, pp. 112–123, 2020.

[24] S. Ferdousi, M. Tornatore, F. Dikbiyik, C. U. Martel, S. Xu, Y. Hirota, Y. Awaji, and B. Mukherjee, "Joint progressive network and datacenter recovery after large-scale disasters," *IEEE Transactions on Network and Service Management*, vol. 17, no. 3, pp. 1501–1514, 2020.

[25] M. F. Habib, M. Tornatore, M. De Leenheer, F. Dikbiyik, and B. Mukherjee, "Design of disaster-resilient optical datacenter networks," *J. Lightw. Technol.*, vol. 30, no. 16, pp. 2563–2573, Aug. 2012.

[26] Y. Yin, H. Zhang, M. Zhang, M. Xia, Z. Zhu, S. Dahlfort, and S. Yoo, "Spectral and spatial 2D fragmentation-aware routing and spectrum assignment algorithms in elastic optical networks," *J. Opt. Commun. Netw.*, vol. 5, pp. A100–A106, Oct. 2013.

[27] X. Li, S. Yin, X. Wang, Y. Zhou, Y. Zhao, S. Huang, and J. Zhang, "Content placement with maximum number of end-to-content paths in k-node (edge) content connected optical datacenter networks," *IEEE J. Opt. Commun. Netw*, vol. 9, no. 1, pp. 53–66, Jan. 2017.

[28] M. Ju, "Optimization of protection schemes for next generation optical networks (optimisation de la protection des réseaux optiques de nouvelle génération)," Ph.D. dissertation, Université d'Avignon et des pays de Vauluse, France, 2018.

[29] H. Wu, F. Zhou, Z. Zhu, and Y. Chen, "On the distance spectrum assignment in elastic optical networks," *IEEE/ACM Trans. Netw.*, vol. 25, no. 4, pp. 2391–2404, Aug. 2017.

[30] A. Alleg, T. Ahmed, M. Mosbah, and R. Boutaba, "Joint diversity and redundancy for resilient service chain provisioning," *IEEE Journal on Selected Areas in Communications*, vol. 38, no. 7, pp. 1490–1504, 2020.

[31] I. S. Reed and G. Solomon, "Polynomial codes over certain finite fields," *Journal of the Society for Industrial Applied Mathematics*, vol. 8, no. 2, pp. 300–304, 1960.

[32] R. Gallager, "Low-density parity-check codes," *IRE Transactions on Information Theory*, vol. 8, no. 1, pp. 21–28, 1962.

[33] N. B. El Asghar, I. Jouili, and M. Frikha, "Survivable inter-datacenter network design based on network coding," in *2017 IEEE/ACS 14th International Conference on Computer Systems and Applications (AICCSA)*, 2017, pp. 1192–1197.

[34] Y. Wu, M. Tornatore, C. U. Martel, and B. Mukherjee, "Content fragmentation: A redundancy scheme to save energy in cloud networks," *IEEE Transactions on Green Communications and Networking*, vol. 2, no. 4, pp. 1186–1196, 2018.

[35] L. Xu, M. Lyu, Z. Li, Y. Li, and Y. Xu, "Deterministic data distribution for efficient recovery in erasure-coded storage systems," *IEEE Transactions on Parallel and Distributed Systems*, vol. 31, no. 10, pp. 2248–2262, 2020.

[36] R. Torre, I. Leyva-Mayorga, S. Pandi, H. Salah, G. T. Nguyen, and F. H. P. Fitzek, "Implementation of network-coded cooperation for energy efficient content distribution in 5g mobile small cells," *IEEE Access*, vol. 8, pp. 185 964–185 980, 2020.

[37] S. Liu, K. W. Shum, and C. Li, "Exact-repair codes with partial collaboration in distributed storage systems," *IEEE Transactions on Communications*, vol. 68, no. 7, pp. 4012–4021, 2020.

[38] N. Bao, S. Sahoo, M. Kuang, and Z. Zhang, "Adaptive path splitting based survivable virtual network embedding in elastic optical networks," *Optical Fiber Technology*, vol. 54, p. 102084, 2020.

[39] X. Chen, S. Zhu, L. Jiang, and Z. Zhu, "On spectrum efficient failure-independent path protection p-cycle design in elastic optical networks," *J. Lightw. Technol.*, vol. 33, no. 17, pp. 3719–3729, Sept. 2015.

[40] L. Zhang, W. Lu, X. Zhou, and Z. Zhu, "Dynamic RMSA in spectrum-sliced elastic optical networks for high-throughput service provisioning," in *Proc. Int. Conf. Comput. Netw. Commun.*, Jan. 2013, pp. 380–384.

[41] C. Anglano, R. Gaeta, and M. Grangetto, "Exploiting rateless codes in cloud storage systems," *IEEE Transactions on Parallel and Distributed Systems*, vol. 26, no. 5, pp. 1313–1322, 2015.

[42] T. L. Weems, "How far is far enough," *Disaster Recovery Journal*, vol. 16, no. 2, Spring 2003.